Langmuir
Article
pubs.acs.org/Langmuir

Effect of Microphase Separation on the Protein Resistance of a Polymeric Surface

Chunfeng Ma, Yi Hou, Shi Liu, and Guangzhao Zhang*

Hefei National Laboratory for Physical Sciences at Microscale, Department of Chemical Physics, University of Science and Technology of China, Hefei 230026, China

Received February 25, 2009. Revised Manuscript Received March 13, 2009

Segmented polyurethanes (PUs) containing poly(ethylene glycol) (PEG), poly(propylene glycol), or poly(dimethylsiloxane) soft segments have been prepared by two-step condensation polymerization. Atom force microscopy observation in air and solution indicates that the segmented PU forms a microphase separation on the surface. By use of quartz crystal microbalance with dissipation and surface plasmon resonance, we have investigated the adsorption of fibrinogen, bovine serum albumin, and lysozyme on a surface constructed by such a PU in aqueous solution in real time. Our results reveal that the protein resistance of the PUs arises from the hydrated PEG segments instead of microphase separation.

Introduction

Protein adsorption is significant in protein purification, immobilization of enzymes or antibodies, development of biochips and biosensors, drug delivery, and food and biochemical processing.[1,2] On the other hand, nonspecific protein adsorption induces undesirable results such as biofouling on ship hulls, deposition of blood proteins onto medical devices, and blockage of filtration membranes in bioseparation processes.[3−8] Accordingly, much attention has been paid to the design and development of a surface with protein resistance. The materials used include polysaccharides,[9] heparin,[10,11] zwitterionic compounds,[7,12−16] and poly(ethylene glycol) (PEG).[17,18] In particular, PEG-based materials exhibit good protein resistance and biocompatibility as well as low toxicity.[19,20]

One question in protein adsorption or protein resistance is about the effect of surface morphology. As early as the 1980s, it was reported that the microphase-separated morphology of polyurethane (PU) could profoundly influence the protein−surface interactions and protein adsorption and thereby altered the extent of platelet deposition, activation, and thrombogenesis.[21,22] A surface constructed of PU-containing polybutadiene segments with a moderate microphase separation was also reported to possess a low adsorption ratio of fibrinogen to albumin.[23] Recently, a coating consisting of hyperbranched fluorpolymers crosslinked with PEG was designed for antibiofouling.[24−26] The coating surface with optimal nanoscale topographical and compositional complexities was expected to make protein or glycoprotein adsorption energetically unfavorable and reduce the adhesion strength of the entire organism with the surface. Note that most of the synthetic antifouling materials with microphase separation contain a PEG moiety. Considering that PEG is of protein resistance, the role of microphase separation is difficult to clarify.

It is known that PU consisting of hard and soft segments exhibits a microphase-separated structure; we have prepared PU containing PEG, poly(propylene glycol) (PPG), or poly(dimethylsiloxane) (PDMS) soft segments in the present work (Scheme 1). The PUs can form microphase separation at different levels. On the other hand, quartz crystal microbalance with dissipation (QCM-D)[27,28] and surface plasmon resonance (SPR)[29,30] are sensitive to detect the behavior of a layer at the interface. By use of QCM-D and SPR, we have investigated the effect of microphase separation on the adsorption of fibrinogen, bovine

*To whom correspondence should be addressed.

(1) Glomm, W. R.; Halskau, O.; Hanneseth, A. D.; Volden, S. *J. Phys. Chem. B* **2007**, *111*, 14329.
(2) Oroszlan, P.; Blanco, R.; Lu, X. M.; Yarmush, D.; Karger, B. L. *J. Chromatogr. A* **1990**, *500*, 481.
(3) Ostuni, E.; Chapman, R. G.; Holmlin, R. E.; Takayama, S.; Whitesides, G. M. *Langmuir* **2001**, *17*, 5605.
(4) Kane, R. S.; Deschatelets, P.; Whitesides, G. M. *Langmuir* **2003**, *19*, 2388.
(5) Chang, Y.; Chen, S. F.; Yu, Q. M.; Zhang, Z.; Bernards, M.; Jiang, S. Y. *Biomacromolecules* **2007**, *8*, 122.
(6) Senaratne, W.; Andruzzi, L.; Ober, C. K. *Biomacromolecules* **2005**, *6*, 2427.
(7) Chen, S. F.; Zheng, J.; Li, L. Y.; Jiang, S. Y. *J. Am. Chem. Soc.* **2005**, *127*, 14473.
(8) Metzke, M.; Bai, J. Z.; Guan, Z. B. *J. Am. Chem. Soc.* **2003**, *125*, 7760.
(9) McArthur, S. L.; Mclean, K. M.; Kingshott, P.; St John, H. A. W.; Chatelier, R. C.; Griesser, H. J. *Colloids Surf., B* **2000**, *17*, 37.
(10) Klement, P.; Du, Y. J.; Berry, L.; Andrew, M.; Chan, A. K. C. *Biomaterials* **2002**, *23*, 527.
(11) Johnell, M.; Larsson, R.; Siegbahn, A. *Biomaterials* **2005**, *26*, 1731.
(12) Holmlin, R. E.; Chen, X. X.; Chapman, R. G.; Takayama, S.; Whitesides, G. M. *Langmuir* **2001**, *17*, 2841.
(13) Chang, Y.; Chen, S. F.; Zhang, Z.; Jiang, S. Y. *Langmuir* **2006**, *22*, 2222.
(14) Zhang, Z.; Chao, T.; Chen, S. F.; Jiang, S. Y. *Langmuir* **2006**, *22*, 10072.
(15) Zhang, Z.; Chen, S. F.; Chang, Y.; Jiang, S. Y. *J. Phys. Chem. B* **2006**, *110*, 10799.
(16) Cho, W. K.; Kong, B.; Choi, I. S. *Langmuir* **2007**, *23*, 5678.
(17) Prime, K. L.; Whitesides, G. M. *J. Am. Chem. Soc.* **1993**, *115*, 10714.
(18) Roberts, C.; Chen, C. S.; Mrksich, M.; Martichonok, V.; Ingber, D. E.; Whitesides, G. M. *J. Am. Chem. Soc.* **1998**, *120*, 6548.
(19) Alcantar, N. A.; Aydil, E. S.; Israelachvili, J. N. *J. Biomed. Mater. Res.* **2000**, *51*, 343.
(20) Harris, J. M. *Poly(ethylene glycol) Chemistry: Biotechnical and Biomedical Applications*; Plenum Press: New York, 1992.
(21) Okana, T.; Nishiyama, S.; Shinohara, I. *J. Biomed. Mater. Res.* **1981**, *15*, 393.
(22) Takahara, A.; Tashita, J.; Kajiyama, T.; Takayanagi, M. *Polymer* **1985**, *26*, 978.
(23) Huang, S. L.; Chao, M. S.; Ruaan, R. C.; Lai, J. Y. *Eur. Polym. J.* **2000**, *36*, 285.
(24) Brown, G. O.; Bergquist, C.; Ferm, P.; Wooley, K. L. *J. Am. Chem. Soc.* **2005**, *127*, 11238.
(25) GudiPati, C. S.; Finlay, J. A.; Callow, J. A.; Callow, M. E.; Wooley, K. L. *Langmuir* **2005**, *21*, 3044.
(26) Bartels, J. W.; Cheng, C.; Powell, K. T.; Xu, J. Q.; Wooley, K. L. *Macromol. Chem. Phys.* **2007**, *208*, 1676.
(27) Höök, F.; Kasemo, B.; Nylander, T.; Fant, C.; Sott, K.; Wlwing, H. *Anal. Chem.* **2001**, *73*, 5796.
(28) Cao, Z.; Du, B. Y.; Chen, T. Y.; Li, H. T.; Xu, J. T.; Fan, Z. Q. *Langmuir* **2008**, *24*, 5543.
(29) Wang, Q.; Wang, J. P.; Geil, P. H.; Padua, G. W. *Biomacromolecules* **2004**, *5*, 1356.
(30) Rich, R. L.; Myszka, D. G. *J. Mol. Recognit.* **2008**, *21*, 355.

Scheme 1. Chemical Structure of a PU with PEG, PPG, or PDMS as the Soft Segments

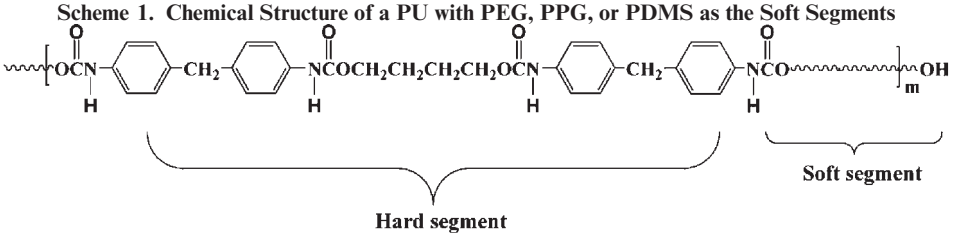

serum albumin (BSA), and lysozyme in real time, where the proteins have different sizes and charging levels. Our aim is to explore what determines the protein adsorption or resistance.

Experimental Section

Materials. PEG (M_w = 2000 g/mol) was obtained from Aldrich. PPG (M_w = 2000 g/mol), PDMS (M_w = 4200 g/mol), 4,4′-diphenylmethane diisocyanate (MDI), 1,4-butane diol (1,4-BD), and dibutyltindilaurate (DBT) were all purchased from Alfa. PEG, PPG, and PDMS were dried under reduced pressure for 2 h prior to use. Tetrahydrofuran (THF) was refluxed over CaH_2 and distilled. Fibrinogen (fraction I from human plasma, M_w = 340 kDa, pI = 5.5) from Merck Chemicals, lysozyme via chicken egg white (M_w = 14.7 kDa, pI = 11.1) from Sangon (Shanghai), and BSA (M_w = 68 kDa, pI = 4.8) from Hualvyuan Biotechnology Company were used as received. Physiological phosphate-buffered saline (PBS, 0.14 M, pH 7.4) was prepared by dissolving NaCl, KCl, Na_2HPO_4, and KH_2PO_4 in Milli-Q water. Each protein solution (1.0 mg/mL) was prepared by dissolving the protein in PBS buffer. Other reagents were used as received.

Sample Preparation. PUs were synthesized via a two-step condensation reaction in THF under a nitrogen atmosphere. MDI reacted with macroglycol at 70 °C for 40 min yielding a low molecular weight prepolymer with the latter as the soft segment. Subsequently, 1,4-BD and DBT were added as the chain extender and catalyst, respectively, and the mixture was reacted at 70 °C for 3 h. The resulting polymers were precipitated in methanol and vacuum-dried for 24 h. The soft segment consists of PEG, PPG, or PDMS. The hard segment is composed of MDI and 1,4-BD. The hard segment content in PEG-based PUs was varied from 23 to 50 wt % so that microphase separation at different scales was obtained. The description of all PUs is shown in Table 1. The film for atomic force microscopy (AFM), QCM-D, or SPR measurements was prepared by spin-casting of a PU solution in THF (0.5 wt %) on a spin coater (CHEMAT, KW-400) at 4000 rpm in air, and the film was heated at 40 °C for 24 h in an oven before use.

AFM Imaging. The height and phase images were conducted on a multimode AFM (Digital Instruments) using a tapping mode.[31] In the height imaging, the cantilever scans horizontally on the plate oscillating at a given frequency so that the oscillation amplitude or the height holds a constant by moving the substrate plate vertically. The vertical movement of the plate is converted to the image of the asperity of the substrate surface. In the phase imaging, considering that the phase shift is sensitive to the local surface property, the height is always kept constant by the height imaging procedure, and the phase shift of the cantilever oscillation is converted into an image. Height and phase signals in air were recorded simultaneously with a standard silicon tapping tip on a beam cantilever. The spring constant of the cantilever was between 20 and 100 N/m, and the nominal radius of curvature of a new tip was between 5 and 10 nm. The cantilever length was 125 μm, and the resonance frequency was 200−400 kHz. The surface morphology in solution was also observed by using an AFM equipped with an OMCL-TR800PSA tip (Olympus, Tokyo) and liquid tip holder. The film casted on AT-cut quartz crystal was equilibrated in PBS buffer for 12 h and attached on the sample holder before the measurement. PBS buffer was added into the space between the sample and the tip holder with a syringe, and the scanning of the tip commenced at a resonance frequency of 7−9 KHz. All of the measurements were carried out at 25 °C. The data were analyzed with Nanoscope III software.

Table 1. Composition of the PUs

sample	soft segment	MDI/macroglycol/chain extender[a]	hard segment content (wt %)[b]
PEG-PU23	PEG2000	2:1:1	23
PEG-PU30	PEG2000	3:1:2	30
PEG-PU40	PEG2000	5:1:4	40
PEG-PU50	PEG2000	7:1:6	50
PPG-PU23	PPG2000	2:1:1	23
PDMS-PU23	PDMS4200	4:1:3	23

[a] Feed molar ratio. [b] The total weight percentage of MDI and 1,4-BD.

QCM-D Measurements. QCM-D and the AT-cut quartz crystal with a fundamental resonant frequency of 5 MHz were from Q-sense AB.[32] When a quartz crystal is excited to oscillate in the thickness shear mode at its fundamental resonant frequency (f_0) by applying a RF voltage across the electrodes near the resonant frequency, the addition of a small layer to the electrodes leads to a decrease in resonant frequency (Δf) which is proportional to the mass (Δm) of the layer. In vacuum or air, if the layer is rigid, evenly distributed, and much thinner than the crystal, Δf is related to Δm and the overtone number (n = 1, 3, 5...) by the Sauerbrey equation[33]

$$\Delta m = -\frac{\rho_q l_q}{f_0}\frac{\Delta f}{n} = -C\frac{\Delta f}{n} \quad (1)$$

where f_0 is the fundamental frequency, ρ_q and l_q are, respectively, the specific density and thickness of the quartz crystal, and C (= 17.7 ng/cm^2 Hz) is the constant of the crystal. The dissipation factor is defined by

$$\Delta D = \frac{E_d}{2\pi E_s} \quad (2)$$

where E_d is the energy dissipated during one oscillation and E_s is the energy stored in the oscillating system. The measurement of ΔD is based on the fact that the voltage over the crystal decays exponentially as a damped sinusoidal when the driving power of a piezoelectric oscillator is switched off. By switching the driving voltage on and off periodically, we can simultaneously obtain a series of the changes of the resonant frequency and the dissipation factor. The quartz crystal is mounted in a fluid cell with one side exposed to the solution. The measurable frequency shift is within ±1 Hz in aqueous medium. The effect of surface roughness can be neglected since the highly polished crystal has a root-mean-square roughness less than 3 nm.[34]

(31) Ishida, N.; Inoue, T.; Miyahara, M.; Higashitani, K. *Langmuir* **2000**, *16*, 6377.

(32) Rodahl, M.; Hook, F.; Krozer, A.; Kasemo, B.; Breszinsky, P. *Rev. Sci. Instrum.* **1995**, *66*, 3924.

(33) Sauerbrey, G. *Z. Phys.* **1959**, *155*, 206.

(34) Daikhin, L.; Urbakh, M. *Faraday Discuss.* **1997**, *107*, 27.

In the present study, PBS buffer was used as the reference for protein adsorption measurement. Upon protein adsorption to the crystal surface, the frequency shift is due to the mass change of the protein and the water bound and adsorbed on the protein layer. Because of the viscoelastic contribution of the protein layer and the hydration effects, such mass can not relate to the frequency shift via Sauerbrey equation. However, as the first approximation, the Sauerbrey equation can qualitatively describe the relation between the mass and the frequency shift; namely, the mass increases as the frequency shift decreases.[27,35] All of the results presented here are those from the third overtone ($n = 3$). The values of Δf and ΔD measured from the fundamental frequency were discarded because they are usually noisy due to the insufficient energy trapping.[36] The results from the fifth and seventh overtones were not presented since they were similar to those from the third overtone. All of the experiments were performed at 25 °C.

SPR Measurements. SPR measurements were carried out on Biacore X at 25 °C. The gold-coated glass plate was attached to a glass prism ($n \approx 1.65$) with a silicone opto-interface between them so that they matched in refractive index.[37,38] The response was linear to the added mass of the layer with 1000 RU $\approx$ 1 ng/mm^2, where RU was the response unit (RU).[39] Light from a near-infrared light-emitting diode was focused through the prism on to the sensor surface in a wedge-shaped beam to give a fixed range of incident light angle. Light reflected from the sensor was monitored by a linear array of light-sensitive diodes with a resolution of ~0.1°. The protein solution was delivered to the surface at a flow rate of 10 μL/min. The amount of protein adsorbed designated as the change in RUs (ΔRU) was determined by subtracting the RU value for the reference from that for the protein solution.

Results and Discussion

Figure 1 shows the AFM image of PEG-PU23 observed in air. The surface has topography with a lateral dimension of ~100 nm and height of ~10 nm. The phase image clearly shows the microphase-separated structure, where the brighter part corresponds to the larger phase lag region. Taking into consideration the occupied area, we can reasonably attribute the darker matrix and brighter domains to the hard and soft segments, respectively.[40]

To investigate the effect of microphase separation at different scales, we have prepared PEG-PU with the same soft segments (PEG) but different hard segments contents. Figure 2a−d shows that the domain size of PEG-PU decreases from 100 to 10 nm as the hard segment content is varied from 23 to 50 wt % in air. This is understandable. The formation of the microphase-separated structure of PU is closely related to the hard segments with a high crystallizability.[40,41] As the hard segment content increases, the crystallization increases.[42] Thus, the hard and soft segments become more immiscible, leading to a larger degree of microphase separation. Figure 2e,f shows that PPG-PU23 and PDMS-PU23 also have microphase-separated surfaces with a domain of 30 and 50 nm, respectively. Note that PDMS-PU23 exhibits the largest interdomain in all of the PUs studied. This is because PDMS with a low surface energy can migrate to the surface.[43]

Figure 3a−d shows the phase images of PEG-PUs with different hard segment contents observed in PBS. The size of the phase domain ranges from 200 to 50 nm as the hard segment content increases. In addition, the PPG-PU23 and PDMS-PU23 surfaces also exhibit a microphase-separated structure in solution (Figure 3e,f). Clearly, the phase domain increases in size in comparison with that in air. This is probably due to the swelling of the hydrophilic segments and the reorientation of the polymer induced by water.[44,45]

The protein adsorption on the microphase-separated surface was first investigated by QCM-D. Figure 4 shows the time dependence of frequency shift (Δf) and energy dissipation shift (ΔD) for the adsorption of fibrinogen on different PU surfaces, where fibrinogen is a large blood plasma protein. For any PEG-PU surface, only small shifts in Δf and ΔD can be observed after the introduction of the fibrinogen solution. Δf and ΔD return to the baselines after rinsing with PBS. As stated above, Δf is related to the mass on the sensor surface, whereas ΔD is related to the thickness and viscoelasticity of the polymer layer. Clearly, no fibrinogen is adsorbed on any PEG-PU surface. The small shifts of Δf and ΔD before rinsing can be attributed to the change in the viscosity and density of the solution when PBS is replaced by the fibrinogen solution. Because the proteins are not adsorbed on PEG-PU with any microphase separation scale that we investigated, the protein resistance is not affected by microphase separation.

For PPG-PU23 with the same hard segment content as PEG-PU23, the size of the microphase-separated domains is ~30 nm. When fibrinogen solution is introduced, Δf decreases and ΔD increases sharply. Subsequently, Δf and ΔD gradually vary and level off, indicating the saturation of surface. After rinsing with PBS, Δf and ΔD show a marked change in comparison with those before the fibrinogen solution is introduced, indicating that PPG-PU23 can adsorb fibrinogen although PPG has only one more methylene in each monomeric unit in comparison with PEG. We also examined the adsorption of fibrinogen on a pure PPG surface without any microphase separation. Obviously, the PPG surface can adsorb fibrinogen, and the adsorption quantity is close to that on PPG-PU23 surface. Therefore, the adsorbability of PPG arises from its nature instead of microphase separation. In other words, the nature of PEG is responsible for its protein resistance.

It is known that the PDMS surface has a high interfacial energy with water.[46] PDMS-based materials have been widely used as a fouling release coating because their low modulus and low surface energy allow the adhered organism to easily detach from the surface. Figure 4 shows that PDMS-PU23 with the same hard segment content as those of PEG-PU23 and PPG-PU23 can adsorb fibrinogen reflecting in the remarked changes in Δf and ΔD after the rinsing. Thus, the low surface energy is not the main reason for protein resistance.

Figure 5 shows the time dependence of frequency shift (Δf) and energy dissipation shift (ΔD) for the adsorption of BSA on different PU surfaces. BSA with a smaller size than fibrinogen is the most abundant protein in blood. For PEG-PU with different hard segment contents, Δf and ΔD slightly change after

(35) Voinova, M. V.; Jonson, M.; Kasemo, B. *Biosens. Bioelectron.* **2002**, *17*, 835.
(36) Bottom, V. E. *Introduction to Quartz Crystal Unit Design*; Van Nostrand Reinhold Co.: New York, 1982.
(37) Kretschmann, E.; Raether, H. *Z. Naturforsch., A* **1968**, *23*, 2135.
(38) Liedberg, B.; Nylander, C.; Lunstrom, I. *Sens. Actuators* **1983**, *4*, 299.
(39) Stenberg, E.; Persson, B.; Poss, H.; Urbaniczky, C. *J. Collioid Interface Sci.* **1991**, *143*, 513.
(40) Kojio, K.; Uchiba, Y.; Mitsui, Y.; Furukawa, M.; Sasaki, S.; Matsunaga, H.; Okuda, H. *Macromolecules* **2007**, *40*, 2625.
(41) Blackwell, J.; Lee, C. D. *J. Polym. Sci. Polym. Phys. Ed.* **1984**, *22*, 759.
(42) Nakamae, K.; Nishino, T.; Asaoka, S.; Sudaryanoto *Int. J. Adhes. Adhes.* **1996**, *16*, 233.
(43) Chen, X.; Gardella, J. A.Jr.; Ho, T.; Wynne, K. J. *Macromolecules* **1995**, *28*, 1635.
(44) Kim, J. H.; Kim, S. C. *Macromolecules* **2003**, *36*, 2867.
(45) Agnihotri, A.; Garrett, J. T.; Runt, J.; Siedlecki, C. A. *J. Biomater. Sci. Polym. Ed.* **2006**, *17*, 227.
(46) Krishnan, S.; Weinman, C. J.; Ober, C. K. *J. Mater. Chem.* **2008**, *18*, 3405.

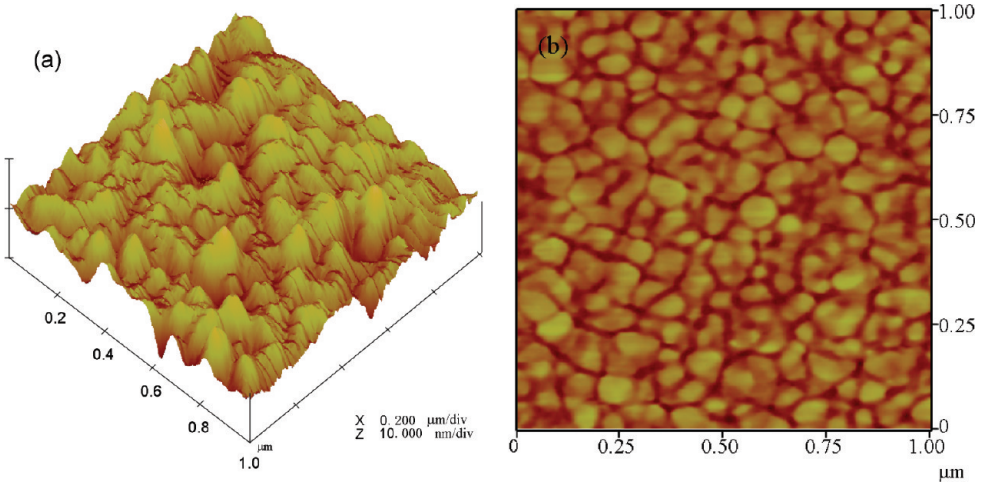

Figure 1. AFM height images (a) and phase images (b) of PEG-PU23 in air.

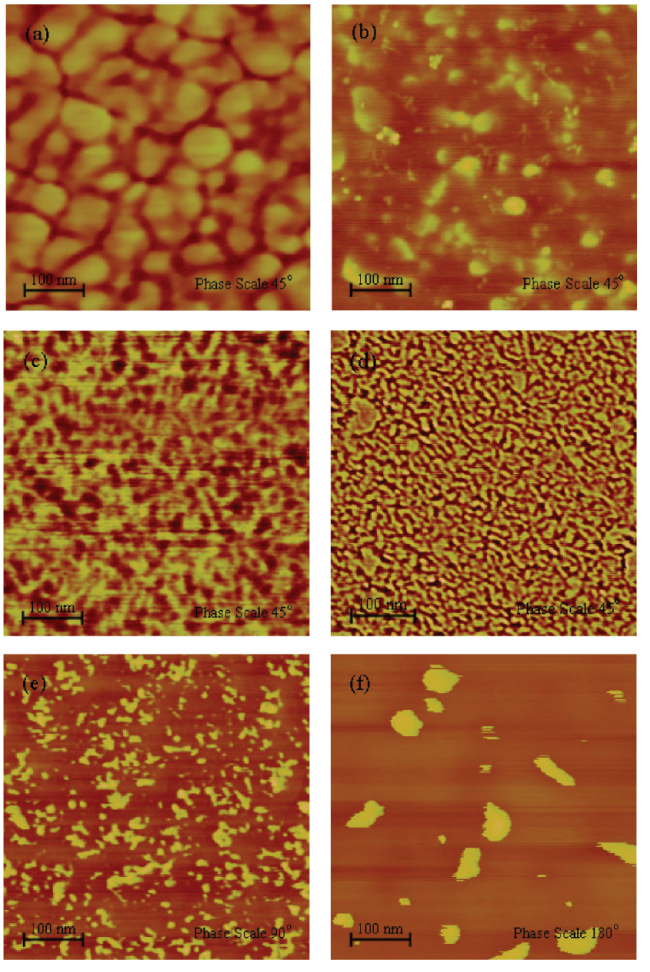

Figure 2. AFM phase images of PU surfaces in air. (a) PEG-PU23, (b) PEG-PU30, (c) PEG-PU40, (d) PEG-PU50, (e) PPG-PU23, and (f) PDMS-PU23.

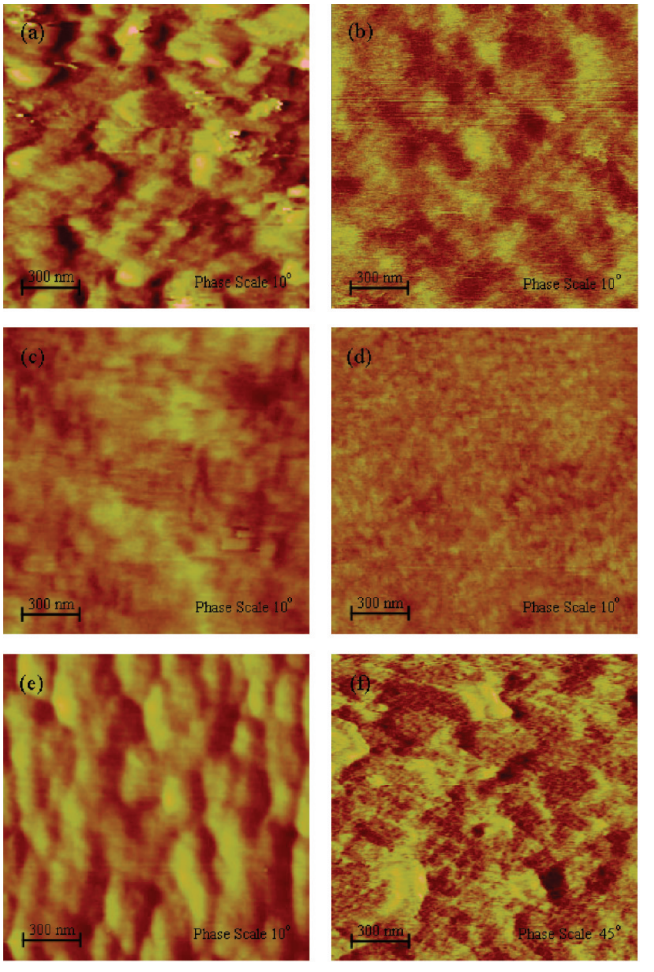

Figure 3. AFM phase images of PU surfaces in PBS (0.14 M, pH 7.4). (a) PEG-PU23, (b) PEG-PU30, (c) PEG-PU40, (d) PEG-PU50, (e) PPG-PU23, and (f) PDMS-PU23.

the BSA solution is introduced, indicating that almost no BSA is adsorbed on the surface. For pure PPG, PPG-PU23, and PDMS-PU23, Δf values decrease and ΔD values increase markedly, indicating the adsorption of BSA on the surfaces.

Figure 6 shows the time dependence of frequency shift (Δf) and energy dissipation shift (ΔD) for the adsorption of lysozyme on different PU surfaces. Lysozyme has the smallest size in the three proteins studied, and it is positively charged under the experimental conditions (PBS, 0.14 M, pH 7.4). Similar to fibrinogen and BSA, lysozyme is not adsorbed on PEG-PUs regardless of the different microphase separation, reflecting the slight changes of Δf and ΔD before and after the lysozyme solution is introduced. In contrast, for PPG-PU23 and PDMS-PU23 surfaces, the marked decrease in Δf and increase in ΔD indicate that lysozyme is adsorbed on the surfaces even though they have a microphase-separated structure.

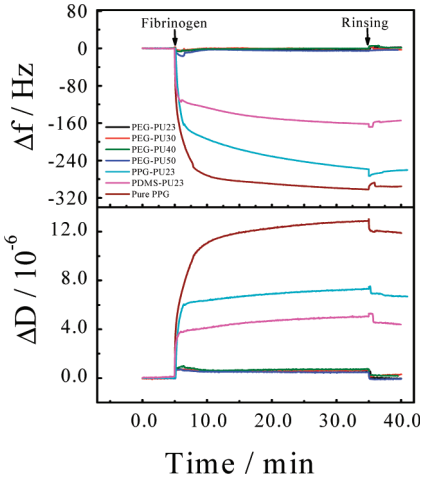

Figure 4. Time dependence of frequency shift (Δf) and energy dissipation shift (ΔD) for the adsorption of fibrinogen on a PU surface at 25 °C.

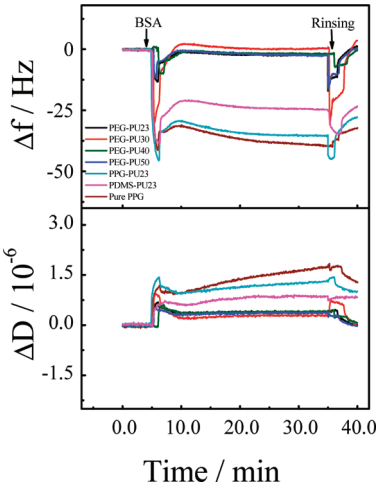

Figure 5. Time dependence of frequency shift (Δf) and energy dissipation shift (ΔD) for the adsorption of BSA on a PU surface at 25 °C.

The protein adsorption on the microphase-separated surface was also investigated by SPR. Figure 7 shows SPR sensorgrams for the fibrinogen adsorption onto the surfaces of different PUs. After the addition of the fibrinogen solution, a rapid increase in the SPR signal can be observed. This increase is caused by the change in refractive index because of the replacement of the PBS with a protein solution and the adsorbed protein.[47] When the surface is rinsed with PBS, the SPR response (ΔRU) for each PEG-PU is less than 50 RU or ~0.05 ng/mm^2 regardless of the microphase separation scale, indicating a low adsorption of fibrinogen. For PPG-PU23, PDMS-PU23, and pure PPG, the measured ΔRU values are ~1800, 1390, and 2200 RU, respectively, indicating that the surfaces can adsorb fibrinogen. Similar results can be obtained in the cases of the adsorption of BSA and lysozyme on the above PU surfaces (Figures 8 and 9).

SPR studies further demonstrate that PEG-PUs with different microphase separation have resistance to the three proteins, whereas PPG-PU and PDMS-PU are able to adsorb the proteins even though they have a microphase-separated surface. Thus, microphase separation is not responsible for the protein resistance.

(47) Stenberg, E.; Persson, B.; Ross, H.; Urbaniczky, C. *J. Colloid Interface Sci.* **1991**, *143*, 513.

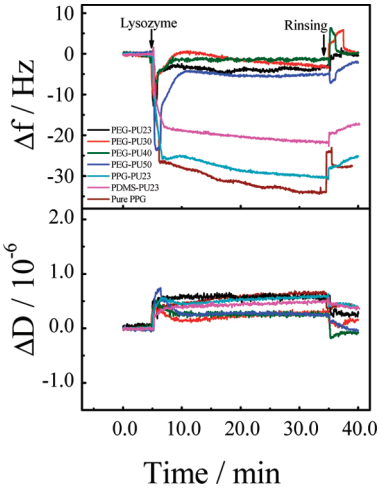

Figure 6. Time dependence of frequency shift (Δf) and energy dissipation shift (ΔD) for the adsorption of lysozyme on a PU surface at 25 °C.

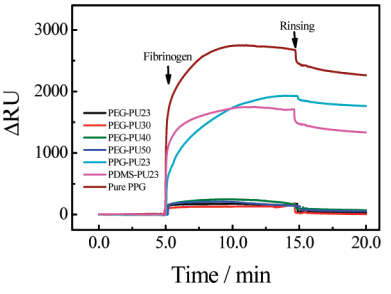

Figure 7. SPR sensorgrams for the adsorption of fibrinogen on a PU surface at 25 °C.

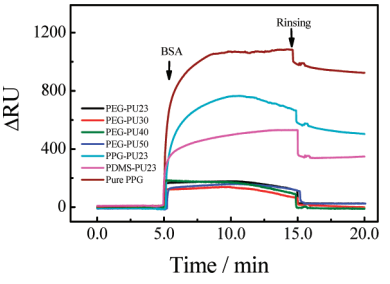

Figure 8. SPR sensorgrams for the adsorption of BSA on a PU surface at 25 °C.

Note that hard segments in all of the PUs consist of MDI and 1,4-BD; the difference in protein adsorption should arise from the different nature or properties of the soft segments. Besides, because PPG used here has a lower critical solution temperature (LCST) below 25 °C,[48] the protein adsorption of PPG-PU or PDMS-PU should be due to the hydrophobic interactions between the surface and the proteins. Therefore, the protein resistance of PEG should relate to its hydrophilicity or hydration. Actually, the mechanism of the protein resistance of PEG remains unclear. In a steric repulsion model, the protein resistance is attributed to the compression or the conformational entropy loss of PEG chains as the protein approaches the surface, which leads to repulsive protein−PEG interactions.[49] Computer simulations

(48) Chen, J.; Spear, S. K.; Huddleston, J. G.; Rogers, R. D. *Green Chem.* **2005**, *7*, 64.

(49) Jeon, S. I.; Lee, J. H.; Andrade, J. D.; de Gennes, P. G. *J. Colloid Interface Sci.* **1991**, *142*, 149.

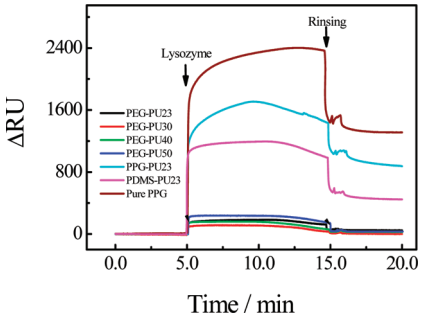

Figure 9. SPR sensorgrams for the adsorption of lysozyme on a PU surface at 25 °C.

further indicate that the density and thickness of the PEG chains have a great effect on the protein resistance.[49,50] This was further confirmed by some experiments.[51−53] However, this model only suits the systems with long PEG chains. For short PEG chains with limited conformational changes, especially the self-assembled monolayers with only a few EG units per molecule, the model is not applicable.[17] The protein resistance of short PEG chains can be interpreted in terms of the water barrier theory, where PEG chains are assumed to create a strong surface hydration layer via hydrogen bonds, forming a physical barrier to prevent direct contact between the protein and the surface.[7] Molecular simulations demonstrate a layer of tightly bound water molecules around oligo(ethylene glycol) (OEG) chains,[54−56] and some experiments also reveal that water at the protein−OEG interface plays an important role in the protein resistance of OEG.[3,57,58]

(50) McPherson, T.; Kidane, A.; Szleifer, I.; Park, K. *Langmuir* **1998**, *14*, 176.
(51) Shalaby, S. W. *Polymers as Biomaterials*; Plenum: New York, 1984.
(52) Gombotz, W. R.; Wang, G. H.; Hoffman, A. S. *J. Appl. Polym. Sci.* **1989**, *37*, 91.
(53) Leckband, D.; Sheth, S.; Halperin, A. *J. Biomater. Sci., Polym. Ed.* **1999**, *10*, 1125.
(54) Pertsin, A. J.; Grunze, M. *Langmuir* **2000**, *16*, 8829.
(55) Zheng, J.; Li, L. Y.; Chen, S. F.; Jiang, S. Y. *Langmuir* **2004**, *20*, 8931.
(56) Zheng, J.; Li, L. Y.; Tsao, H. K.; Sheng, Y. J.; Chen, S. F.; Jiang, S. Y. *Biophys. J.* **2005**, *89*, 158.
(57) Li, L. Y.; Chen, S. F.; Zheng, J.; Ratner, B. D.; Jiang, S. Y. *J. Phys. Chem. B* **2005**, *109*, 2934.
(58) Heuberger, M.; Drobek, T.; Vörös, J. *Langmuir* **2004**, *20*, 9445.

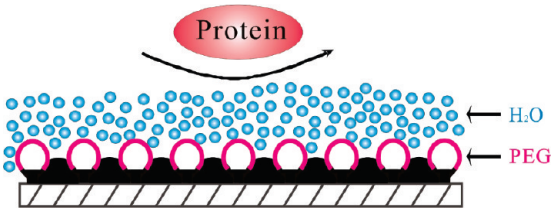

Figure 10. Schematic illustration for the protein resistance of PEG-PUs.

In the present study, because the short PEG segments are confined between the hard segments, their conformational change is limited. Obviously, the protein resistance of PEG-PUs should not arise from the steric repulsion but hydration layer. Note that although the microphase separation does not directly result in the protein resistance, the microphase-separated structure leads PEG segments to be exposed to water molecules so that the hydration layer around PEG segments can form. This is favorable to the protein resistance. Moreover, the hard segments in the microphase-separated structure improve the mechanical properties of the materials. Figure 10 illustrates the protein resistance of PEG-PUs.

Conclusion

The studies on the protein adsorption of PUs with PEG, PPG, or PDMS soft segments can lead to the following conclusions. A surface constructed by PUs with PPG or PDMS segments can adsorb fibrinogen, BSA, and lysozyme. A surface constructed by PUs with PEG segments exhibit protein resistance due to the formation of hydration layer around PEG segments. Microphase separation is not directly responsible for the protein resistance but may favor the formation of the hydration layer around PEG chains.

Acknowledgment. Financial support from the National Distinguished Young Investigator Fund (20474060) and Ministry of Science and Technology of China (2007CB936401) is acknowledged.